Int. J. Electrochem. Sci., 9 **(2014)** 6734 - 6750

International Journal of ELECTROCHEMICAL SCIENCE
www.electrochemsci.org

Electrochemical Behavior of the Welded Joint Between Carbon Steel and Stainless Steel by Means of Electrochemical Noise

J. T. Pérez-Quiroz[1,2], *E. M. Alonso-Guzmán*[1], *W. Martínez-Molina*[2], *H. L. Chávez-García M. Rendón-Belmonte*[1] , *M. Martínez-Madrid*[1]

[1]Instituto Mexicano del Transporte, Km 12 carretera Querétaro - Galindo S/N, Sanfandila, Pedro Escobedo, 76703, Querétaro, México.
[2]Universidad Michoacana de San Nicolás de Hidalgo, Avenida Francisco J. Múgica S/N Ciudad Universitaria, C.P. 58070, Morelia, Michoacán, México.
*E-mail: jtperez@imt.mx

Received: 9 June 2014 / *Accepted:* 9 September 2014 / *Published:* 29 September 2014

Welding process between dissimilar metals during rehabilitation of damaged structural reinforcement by corrosion, has a number of microstructural changes due to the heat generated at the time of joint. These transformations propitiate the heat affected zone to be more susceptible to damage by corrosion. The present work evaluates the corrosion behavior of the area affected by heat between AISI 304 austenitic stainless steel and A615 carbon steel, by means of the electrochemical noise technique. The results of this technique indicate that the connection between the two steels have sufficient corrosion resistance in an alkaline medium, but not in a saline one. Also, the technique showed the predominant form of corrosion. The results show that the use of stainless steel welded with carbon steel in alkaline medium is possible, which represents the pH of a rehabilitated structure.

Keywords: galvanic corrosion, stainless steel, welding, electrochemical noise, rehabilitation

1. INTRODUCTION

The design of concrete structures has been performed with a mechanical strength method; as a result, the structures have supported the service loads. However, some problems related to the environment in which the structure is located (in the case carbonation of concrete) have arisen, as well as the steel corrosion due to chloride ions and for which data there is no design. Deterioration caused by corrosion has no break and science and technology continue further studies and methodologies to develop stronger materials [1-5]. Research projects on the corrosion phenomenon of reinforced concrete elements becomes an important issue due to the large amount of money spent on repairing,

rebuilding or replacing structures damaged by corrosion [6] despite the fact that a number of hydraulic reinforced concrete works built in the twentieth century are being classified as national artistic assets, which implies the need to preserve and conserve them.

The phenomenon of corrosion of steel in reinforced concrete structures was first recognized in the late 1960s, since then many methods have been developed with the intention of preventing corrosion. These methods can be divided into four different categories depending on the form of protection [3]:

- Alternative reinforcement and re-design of concrete elements
- Barrier Methods
- Electrochemical methods

Cathodic protection by impressed current method (ICCP) [2-3,7-8].

Cathodic protection by sacrificial or galvanic anodes (CPGA) [2-3,7-8].

Corrosion Inhibitors

Electrochemical removal of chloride ions

Electrochemical realkalinisation

- Rehabilitation of reinforced concrete structures with new materials [9].

The purpose of a "repair" is to restore or reinforce a specific property such as: durability, structural strength, functionality, or appearance. The range of rehabilitation techniques is broad and diverse, and some are used on steel and others on concrete, or on both materials [9].

When working on a structure damaged by corrosion, there are three strategies to choose from.

1. The first consists of restoring, which means removing all the damaged parts and replacing them with new materials; thus, representing a large work load and cost.
2. The second strategy consists of maintaining the structure in the original state which is the option commonly adopted since it only involves the application of small patches that prevent corrosion from spreading.
1. The third strategy is to implement treatments capable of maintaining low levels in the corrosion rate of steel.

In the last two cases techniques such as cathodic protection, chloride extraction and realkalisation have had a better acceptance. The fact that concrete structures are corroded and need to be repaired after 10, 20, or 30 years of service, is a reality. Besides, special chapters devoted to durability of concrete structures are increasingly included in the standard regulations [10-11].

In the construction area special steels are normally used, and although this technique is not widespread in Mexico, there are researches on their use in process. For example, the hot dip galvanized steel, which applications in reinforcing steel are used for new concrete elements is still controversial worldwide [12]. Stainless steel has become an attractive alternative when compared to traditional methods of repair; for example, carbon steel, epoxy coatings, corrosion inhibitors, cathodic protection, etc. Besides, it has apparently performed well without causing galvanic effects in the last 20 years. Although the use of these steels usually have very limited applications due to its high cost of production, the benefit in the medium and long terms, will absorb the initial cost. [9,12-14].

For example, in the port located in Progreso, Yucatan, Mexico, there is a pier built between 1937 and 1941, where 304 stainless steel bars were used as reinforcement and rehabilitation has not been necessary so far. In contrast, another dock built in 1960 in the same place where carbon steel rebar were used, is completely destroyed. [12]

Figure 1. Stainless steel built dock on the right side, carbon dock on the left side of the image [12].

The AISI 304 austenitic stainless steel is resistant to corrosion in concrete even in cases with a high content of chloride ion. Repairs include the selective replacement of carbon steel with stainless steel in critical areas. There are three methods to connect stainless steel with carbon steel: not welded couplings, welded couplings, and mechanical connectors. Typically the stainless steel can be welded on site, but often the binding capacity of welded carbon steel bars existing is questionable and in some cases unknown.

Therefore, welding on site is not always possible. The corrosion resistance of the stainless steel is reduced due to the welding process and the contamination with iron depositions of tools used. Stainless steels can be attacked by various agents. However, this attack is much slower than in the case of carbon steel, which due to its low carbon content and high chromium content is less prone to precipitation carbides in the critical temperature range, so its use is recommended for the construction of welded equipment [14-15].

Suggesting the study of different materials for the rehabilitation of concrete structures is a very important issue, for it can benefit highly relevant factors such as increased corrosion resistance of the rehabilitated area as well as the conservation of their mechanical properties. Thus, ensuring a longer life of the repaired area and, as a consequence, of the structure. Theoretically, the contact of stainless steel with a less noble metal such as carbon steel, may lead to galvanic type corrosion which will depend on the area ratio between carbon steel and stainless steel. Still, the bond between stainless steel and carbon steel should not promote significant galvanic corrosion as it has a poor performance as the cathode [14].

The study of electrochemical noise records the noise generated by oscillations of current and electrochemical potential. In this regard, the metal / electrolyte interface is the point where the signals in the form of small variations (transients) in the potential and current are produced and they are associated with the charge transfer processes occurring. [16-17].

The phenomena of localized corrosion, such as pitting and crevice corrosion, are electrochemical stochastic processes related to activation and repassivation of the metal / electrolyte

interface and represent an important source of electrochemical noise. Indeed, this is the area where the (RE) technique has experienced its greatest advance and has allowed a unique form of registration of submicroscopic processes that start these forms of corrosion [17].

Thus, variations in potential and current registered as electrochemical signals derived from the stochastic metal dissolution, caused, firstly, by different energy sites on the surface associated with heterogeneities of the materials [18] such as:

- Segregations
- Impurities
- Phases with different chemical composition
- Thermal and mechanical treatments
- Anisotropies or defects in the crystal structure

Other factors that are considered important in electrochemical noise generation are [19]:

- Evolution of hydrogen
- Changes in mass transport rate
- Ion exchange and atoms on the surface as a consequence of the dynamic equilibrium of metal and the medium
- Micro-crack spreading
- Initiation of pitting, metastable pitting and stable pitting growth
- Friction and abrasion
- Phenomena associated with passive systems

2. EXPERIMENTAL DEVELOPMENT

2.1 Equipment and Materials

Table 1. Materials, equipment, chemical solutions used during the development of research.

Materials	**Equipment (hardware)**	**Solutions**
➢ **ASTM A615 carbon steel rods [20]** ➢ **AISI 304 austenitic stainless steel rods** ➢ **Coated electrode E309L-16** ➢ **Steel Grinding number 180-1000** ➢ **Alumina Al_2O_3 of 1, 0.5 and 0.3 microns** ➢ **500 ml beakers** ➢ **Cork stopper No.14** ➢ **Wire No. 12 gauge**	➢Eutectic Castoli Master NT2000 Welding Plant, ➢ Maximat Lathe Super 1 ➢FUHO (MPC-F-300) Vertical saw ➢Chevalier-1224AD Grinding machine ➢ Jean Wirtz Double Disc Sander ➢ Jean Wirtz TG250 Double Disc Blaster ➢ Reference electrode: (saturated calomel electrode) ➢Olympus inverted stage microscope ➢ Brymen Multimeter ➢ ACM GILL Potentiostat ➢hp Computer for data acquisition	➢ Nital ➢ Aqua regia: 1% vol HCl, 1% vol H(NO) $_3$, 1% vol Distilled H_2O. ➢ Sodium chloride (NaCl) 3.5% weight ➢ Calcium hydroxide (saturated) ($Ca(OH)_2$)

Table 1 lists the materials and equipment used during the manufacturing process and evaluation of welded test specimens.

Table 2 specifies the chemical composition of the base metals and filler used for the manufacture of test specimens.

Table 2. Chemical composition of materials wt%

AISI 304 Stainless Steel									
Fe	C	Si	Mn	P	S	Cr	Mo	Ni	Cu
70.34	0.022	0.37	1.32	0.030	0.025	18.35	0.28	8.07	0.41
ASTM A 615 Carbon Steel									
Fe	C	Si	Mn	P	S	Cr	Mo	Ni	Cu
98.7	0.24	0.18	0.74	0.027	0.036	0.085	0.025	0.084	0.02
Chemical composition of the electrode 309L-16									
Fe	C	Si	Mn	P	S	Cr	Mo	Ni	Cu
60.5	0.030	0.50	1.0	0.2	0.2	23.5	0.25	13.5	-

2.2 Fabrication of test specimens.

20 pieces of stainless steel and 20 of carbon steel were cut to the length of 10 cm and diameter of 1.27 cm. One of the rod's end was sharpened to form a bevel pencil tip type with an angle of 30˚ in each stainless steel and carbon steel rods, Figure 2.

Figure 2. Stainless steel and carbon steel bars with an initial length of 100 mm and Ø = 12.7 mm and after manufacturing the 30 ° bevel pencil tip type

The specimens welding process (SMAW) was carried out according to the NMX-H-121-1988 [21] and ANSI/ AWS D1.4-05 [22] standards. A stainless steel coated electrode 309L-16 with the chemical composition shown in Table 2 was used as solder. Also, a Castoli Eutectic Master NT2000 AC/DC welding plant operating during the welding process with 90 amperes. Figure 3 shows the specimens obtaining.

Figure 3. Specimens obtaining Welding process and sharpening of the stainless steel and carbon steel bars.

After welding (SMAW) each of the test specimens were sharpened. The purpose of this process was to remove the excess of solder to obtain a final diameter of 10 mm with a uniform surface finish Figure 3.

A longitudinal cut was made with a vertical bandsaw FUHO (MPC-F-300 model), to expose the welded area of the base metals, and perform the metallographic analysis and corrosion behavior in this area. This operation was performed to obtain identical electrodes in accordance with the ASTM G199 standard [23] and to apply the standard technique of electrochemical noise. Test area was 7 cm^2.

Figure 4. Specimens with longitudinal section.

After cutting the study area of the specimens (figure 4), they were grinded to remove imperfections caused by the vertical cutting saw and leave the surface as smooth as possible. This operation was performed with a Chevalier-1224AD grinding machine.

The metallographic preparation was conducted according to ASTM E 3 [24] standard, the roughing of the samples was carried out with a Jean Wirtz double disc grinder and sandpapers numbers 180, 220, 320, 400, 500 , 600, 800, 1000 and 1200. After roughing, the polishing process was performed in a double disc grinder Jean Wirtz TG250. Alumina (Al_2O_3) with particle size of 1, 0.5 and 0.3 microns (μm) was used as the abrasive agent. During the grinding and polishing processes water was used as lubricant. At the end of the process, the specimens were washed with water and dried with hot air.

In order to reveal the microstructure of carbon steel, it was attacked with Nital 2%.For stainless steel and welded zone a mixture of Nitric acid and Hydrochloric acid (aqua regia) was used [25]. The affected samples are shown in Figure 5.

Figure 5. Specimens chemically attacked. The dark zone shows the carbon steel A615, the clear zone shows the stainless steel AISI 304.

To observe the microstructure metallographic an Olympus inverted stage microscope (PMG3) with an image analyzer (Image-Pro) software was used. The microstructural comparison was made at 20x.

2.3 Corrosion cells making

The corrosion cells for corrosion resistance evaluation of specimens were made with 500 ml beakers, rubber-stoppers and sodium chloride (NaCl) 3.5%/weight and hydroxide calcium ($Ca(OH)_2$) saturated as electrolyte, these solutions were chosen for sodium chloride (NaCl) simulates sea water, and a solution of $Ca(OH)_2$ simulates the concrete alkaline pH which has 12.5 - 13 values (repaired structure).

2.4 Working electrodes

According to ASTM G3 [26] and ASTM G5 [27] standards an electrochemical cell must have three electrodes: working, reference, and auxiliary electrodes. In the case of the electrochemical noise technique, the ASTM G199 [23] standard suggests the use of 2 identical electrodes and one reference electrode. In this case the electrodes are identical specimens which were obtained from the axial section and mirror polished. Recalling that the study area was $7cm^2$ it is worth mentioning that the area ratio between carbon steel/stainless steel was 1:1, and the remaining area was covered with a resin to isolate the medium (electrolyte); thus obtaining the working electrodes.

2.5 Corrosion cells with a sodium chloride (NaCl) and calcium hydroxide solution

A solution with 3.5% / weight sodium chloride (NaCl) in half a liter of distilled water in a beaker and another one with a solution of saturated calcium hydroxide were prepared. A cork stopper

was used 14 as an electrode support. The electrodes were placed in the solutions to simulate the behavior of a repaired area (the area between welded stainless steel and carbon steel in Calcium hydroxide) and in a marine environment (the welded area between stainless steel and carbon steel in sodium chloride).

2.6 Corrosion potential (E_{corr})

The corrosion potential measurement was performed based on the ASTM C-876 [28] standard, prior to the electrochemical noise test in each of the electrodes of electrochemical cells. Corrosion potentials are recorded until stable as established in ASTM G3 [26] and ASTM G5 [27] standards. The corrosion potential measurement was performed with a Brymen multimeter and a reference saturated calomel electrode (SCE).

2.7 Electrochemical noise test

Once the corrosion potential was measured, the electrochemical cells were connected to an ACM Gill potentiostat with Sequencer software 5.1.4 for electrochemical noise testing. The equipment recorded the phenomena oxide - reduction occurring at the electrodes according to ASTM G199 standard [23]. The test conditions were 2048 readings, open circuit potential (OPC).

2.8 Calculation of corrosion rate

Corrosion rate was calculated by the equation of Stern-Geary, using the value of Rn as equivalent to Rp, and the constant B = 0.026 and then using the laws of Faraday corrosion rate values were obtained as ASTM G 59 indicates.

3. RESULTS

3.1 Metallographic analysis

The microstructures are obtained with carbon steel after the welding process. The grain growth at the interface of the welded area and heat affected zone in both base metals is observed, as well as a dendritic growth in the area of the filler material. In both test specimens the welded ASTM A615 carbon steel interface [20] presents grain growth in the area affected by heat (HAZ) and dendritic growth in the welded area. Figure 6 shows the corresponding microstructure as described above.

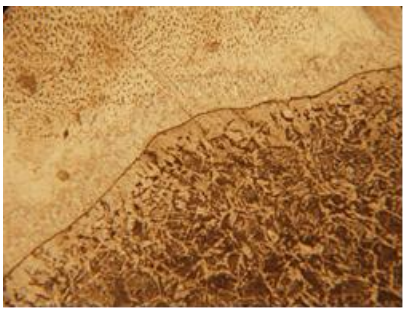

Figure 6. Carbon steel ASTM A615 Interface-welded area photomicrograph taken at 20x.

The interface of austenitic stainless steel AISI 304-welded area presents microstructural changes as a result of the welding process where the welded zone microstructure is dendritic-type. The austenitic matrix stainless steel and the HAZ present some changes in the grain size provoked by the temperature generated during the welding process. The microstructure is shown in Figure 7.

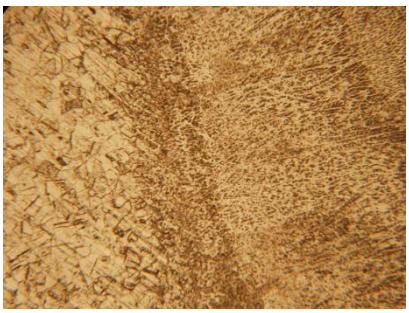

Figure 7. Interface area of AISI 304 austenitic stainless steel -welded area. Photomicrograph taken at 20x.

In Figure 8 the structures obtained after the welding process in the specimens are shown.

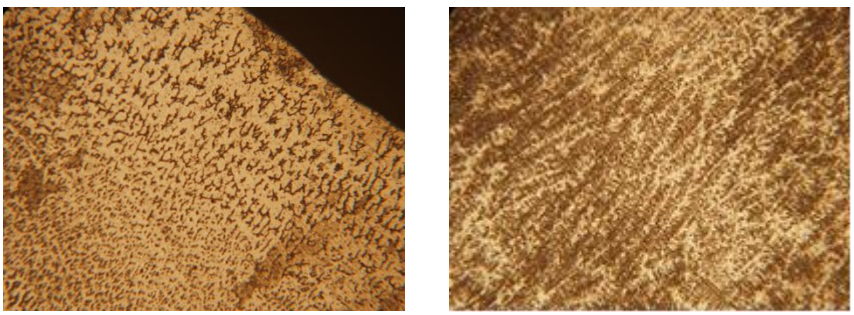

Figure 8. Dendritic microstructure obtained by photomicrograph taken at 20x.

3.2. Potential vs. time of the test specimens in a solution of sodium chloride (NaCl) and calcium hydroxide ($Ca(OH)_2$)

Figure 9 shows the behavior of the corrosion potential values in relation to the time of exposure.

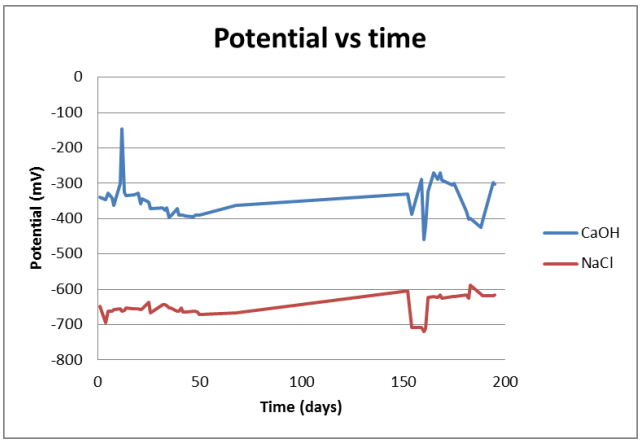

Figure 9. Potential behavior of the specimen vs. time in NaCl solution and $Ca(OH)_2$.

3.3 Results of electrochemical noise technique (EN)

Figure 10 shows the noise resistance values (Rn) of the electrodes in a solution of sodium chloride and calcium hydroxide.

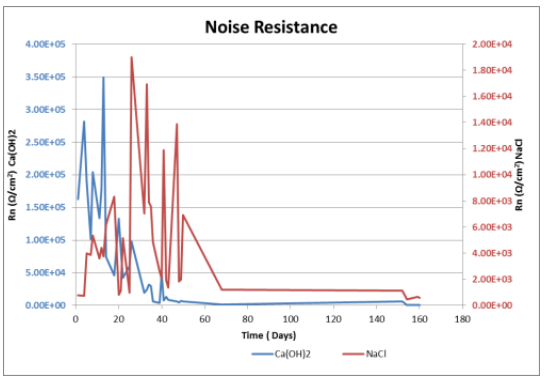

Figure 10. Graph of noise resistance Rn vs. time in the cell of sodium chloride (NaCl).

3.4 Corrosion rate of the steel samples

Figure 11 shows the corrosion rate for two electrochemical cells obtained after 160 days of exposure to solutions. Through these graphs every CR can be compared to each other, and identify the factors that influence these results.

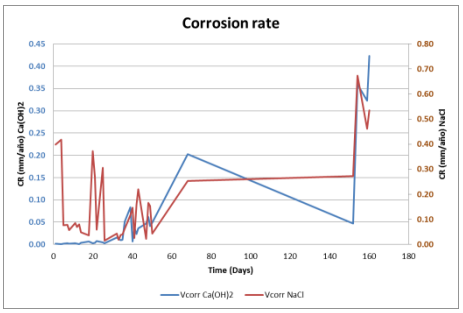

Figure 11. Corrosion rate of the specimens in the test solutions.

3.5 Location Index

The results in terms of location index define the type of corrosion generated on the metal surface. The results are shown in Figure 12 in sodium chloride solution and in calcium hydroxide solution.

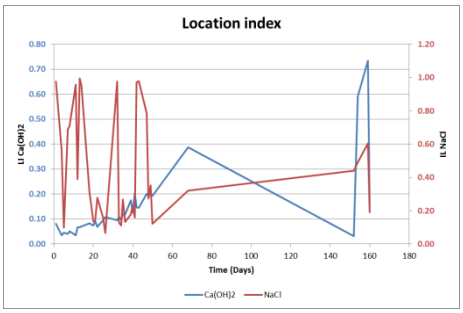

Figure 12. Location index of the specimen exposed to the sodium chloride solution and calcium hydroxide.

4. DISCUSSION OF RESULTS

4.1 Microstructure analysis

The micrographs show that the microstructure obtained is due to the solidification process of the material. The weld is cooled in two phases in the δ ferrite-austenite region. Ferrite becomes increasingly unstable and austenite consumes ferrite through a diffusion controlled reaction. [29]

Figure 13 presents a ferritic-austenitic microstructure (FA) where the ferritic microstructure predominates. In this case solidification starts from the formation of ferrite as a primary phase and during the cooling the solidified remaining liquid is transformed into austenite. Thus, the final microstructure, the primary δ-ferrite phase remains in the nucleus of the dendritic branches, with a vermicular shape, wrapped by austenite [30]. The formation of this microstructure depends on ferrite promoting elements (Cr, Mo) in the absence of austenite promoting elements of (Ni, C, N). [29] So,

because the AISI 304 austenitic stainless steel weight contains 18.35% Chromium, it is likely that this conversion occurs.

The transformations and microstructures shown in Figures 13 and 14 are similar to those reported in the literature 29.

Figure 13. Microstructure with FA (ferritic-austenitic) type dendritic solidification, with not well-defined defined small dendrites. Photomicrograph taken at 20x.

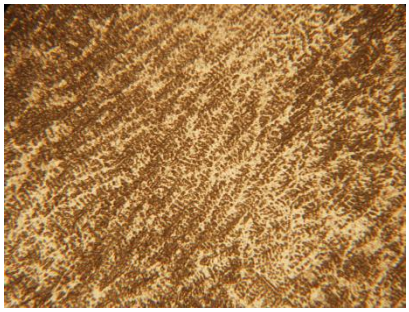

Figure 14. Microstructure with AF (austenitic-ferritic) type dendritic solidification, with well-defined small dendrites. Photomicrograph taken at 20x.

The transformations that have the microstructures of Figures 13 and 14 may be checked in pseudo binary diagram equivalent chromium / nickel equivalent [29], this diagram shows the area in which the formation of the microstructure AF (austenitic-ferritic) type where the dendrite formed shall consist of austenite+ferrite-δ [29]. This formation begins with austenite. At solidifying the remaining liquid its composition is altered becoming rich in ferrite stabilizer. This phase is formed in the interdendritic region at the end of solidification [30]. This happens provided that ferrite stabilizing elements (α) such as chromium (Cr) and molybdenum (Mo) exist [29].

There are four possibilities of solidification and solid state transformations for welding austenitic stainless steels [29].

A and AF: associated with solidification of primary austenite, whereby austenite is the first phase to solidify.

FA and F: The delta ferrite is the primary phase of solidification. Then, a further modification of the microstructure in the solid state occurs.

4.2 Corrosion potential vs. time of the sample in a sodium chloride (NaCl) and calcium hydroxide (Ca (OH) $_2$) solution

The trend of the corrosion potential values with respect to time is between -0632 V to -0663 V vs SCE due to the more active metal is carbon steel (Figure 9), according to ASTM G 82 standard [31]. Since the corrosion potential of carbon steel is precisely of -0.600 V vs. SCE and the stainless steel is -0.400 V vs SCE, the potential values shown in Figure 9 with respect to the ASTM C876 standard indicate that there is a 90% probability of corrosion for they are more negative than -350 V vs SCE [28].

Figure 9 also shows that the value of the corrosion potential is in the range from -0.226 V to -0.396 V vs SCE. These values are associated with the pH of the solution (alkali) and represents a rehabilitated structure, which would justify these potential values. However, in comparison to the ASTM C876 standard [28], the potential range in which most of the values of potential are, indicates that the tendency of the material to corrode is uncertain and is in the range of - 0.200 V to -0.350 V, after a period of time the potential values fall within a range where the probability of corrosion is 90% [28, 32].

4.3 Noise resistance (Nr) of the samples in sodium chloride solution (NaCl) and calcium hydroxide ($Ca(OH)_2$)

Figure 10 shows that the noise resistance values of the test specimen immersed in calcium hydroxide ($Ca(OH)_2$) solution, are lower in comparison to the resistance values of the noise specimen immersed in a solution of sodium chloride (NaCl). The noise resistance values of both specimens indicate that the specimen immersed in the sodium chloride solution is more active; therefore, the corrosion rate is greater in this specimen. The noise resistance values help calculate the corrosion rate, according to the Stern - Geary equation ASTM G 59 [33], ASTM 199 [23].

4.4 Corrosion rates of the specimens in cell. Sodium chloride (NaCl) solution and calcium hydroxide ($Ca(OH)_2$) solution.

In Figure 11 the cell of calcium hydroxide ($Ca(OH)_2$) showed a corrosion rate (CR) relatively low and constant. In the last measuring an increase in the rate of 0.083 mm/year up to day 30 which still remains minimal and in accordance with the criterion of the Durar Network Manual [35] The corrosion rate (CR) is negligible or insignificant, compared to the corrosion rate found in the solution of sodium chloride (NaCl) which rate values are within the criteria of moderate. The rate increases 0.036 mm / year, considered an insignificant corrosion passive state. According to Durar Network Manual [35] values between 0.37 mm / year and 0.4 mm / year are considered as passive or insignificant corrosion. It can be explained because the solution ($Ca(OH)_2$) simulates the pH of 12.5 of a restored concrete structure, and because of the existence of an oxide film that protects the surface of the metal [34]. After day 60, the corrosion rate increases significantly due to a failure in the electrical connection between the copper wire and the base metal as Figure 15 shows.

The specimen immersed in sodium chloride (NaCl) (Figure 11) presents a sudden drop and increase in the corrosion rate (CR) which is a localized corrosion due to the attack of Cl^- ions in the pores that are weak sites of the corrosion product film. This is a continuous attack into the sample [38].

Figure 15. Displays the welded area of the cell with calcium hydroxide. No corrosion products are perceived in the welded joint.

Figure 15 shows that the heat affected zone and base metals show no signs of corrosion because they were immersed in a solution of calcium hydroxide, which simulated a structure restored with stainless steel. Although the joint was made with a (SMAW) welding process, there are no visible corrosion products in the binding stainless steel - carbon steel. Therefore, the high values of corrosion rate found in the cell containing solution of calcium hydroxide are associated with failure in the area where the copper wire was placed and which was covered with epoxy resin and glaze. This insulation was not suitable for in that site the corrosion problem started as seen in Figure 15. This failure is the cause for increases in the corrosion rate; consequently, the experiment was stopped.

4.5 Location index for the samples tested in solutions of sodium chloride (NaCl) and calcium hydroxide ($Ca(OH)_2$)

The location index values obtained for the immersed samples in solution of sodium chloride (NaCl), indicate that the mode of corrosion is localized. This type of corrosion is dominant in the solution of sodium chloride (NaCl), and in the specimen immersed in a solution of calcium hydroxide ($Ca(OH)_2$), the corrosion rate is mixed according to the ASTM G199 standard [23], or with respect to the reference [36-37], the corrosion rate in the specimen immersed in Calcium hydroxide is a combination of localized corrosion and uniform corrosion. ASTM G199 standard [23] indicates that the type of localized corrosion predominates in the range 0.6 to 1.

5. CONCLUSIONS

Based on the information obtained, it can be concluded that the corroded areas to repair concrete structures using stainless steel rods is feasible, even though it is reported that the corrosion resistance decreases in the welded area. In this case the CR values of Figure 11 and visually in Figure 16 confirm that repairing the structure with stainless steel is feasible and corrosion will not occur in the welded joint.

The electrochemical noise technique provides information on the type of predominant corrosion of the metal surface. It also provides information on the corrosion resistance of A615 carbon steel welded joint and AISI 304 austenitic stainless steel. These results show that using stainless steel to rehabilitate structures damaged by corrosion is feasible.

The dendrites microstructure difference of the welded area of test pieces is due to the type of weld solidification and not to the sharpening process. As long as the weld metal of filler solidifies at AF and FA, this phase does not promote corrosion.

The values of the corrosion potential of the cell with calcium hydroxide indicate that the baseline sample is in a passive state and as time passes it changes to an active behavior. In the case of the cell with sodium chloride, the potential indicated that initially the material always remained in the corrosion area according to the ASTM C 876 standard. In this case due to the presence of carbon steel, the electrode follows the most anodic metal behavior.

The electrochemical behavior of welding on dissimilar materials, such as A615 carbon steel-AISI 304 Stainless steel applied to concrete structures, it is stable in terms of corrosion resistance, provided that it maintains its passive state.

The location index values of samples immersed in a solution of sodium chloride (NaCl), indicate that the localized corrosion is the predominant corrosion form. In the specimen immersed in a solution of calcium hydroxide ($Ca(OH)_2$), the rate of corrosion compared to the ASTM G199 standard is mixed; which suggests that the rate of corrosion in the specimen immersed in calcium hydroxide is also a combination of uniform and localized corrosion.

References

1. O. Hernández, C. J. Mendoza. *Ing. Invest. y Tecnol*, 7. 1 (2006) 57.
2. H. Tabatabai, A. Ghorbanpoor, M. D. Pritzl. No. WHRP 09-04 (Wisconsin Highway Research Program), (2009) 7.
3. J. L. Kepler, D. Darwin, C. E. Locke, Jr. Report No. 58, University of Kansas Center for Research, (2000).
4. Vico, W. Morris, M. Vázquez, Institute for Research in Materials Science and Technology (INTEMA), Universidad Nacional de Mar del Plata, (2000).
5. R. Velásquez, M. Acosta, C. Gaona, F. Almeraya, A. Martínez, *Rev. Ing. de Construcción*, 19 (2) (2011) 103-108.
6. F. L. Orantes, A. A. Torres Acosta, J. Terán Guillén, M. Martínez Madrid, *Publicación Técnica* 295 (1) (2006) 11-12.
7. del Valle Moreno, T. Pérez López, M. Martínez Madrid, *Publicación Técnica* 182 (38) (2001) 47.
8. del Valle Moreno, A. A. Torres Acosta, J. Terán Guillén, J. T. Pérez Quiroz, P. Oidor Salinas, *Publicación Técnica*, 290 (2006) 57.
9. F. Gonzalez-Díaz. Doctoral dissertation Realcalinización electroquímica del concreto reforzado carbonatado*:* una opción de prevención contra la corrosión. Universidad Autónoma de Nuevo León and Université Paul Sabatier. (2010).
10. V. Rougier, M. I. Schierloh, R. Souchetti, Proceedings VI Congreso Internacional Sobre Patología y Recuperación de Estructuras *(Cinpar)1* (2010) 1-18.
11. P. Garcés Terradillos, M. A. Climent Llorca, E. Zornoza Gómez, Corrosión de armaduras en estructuras de hormigón armado, Editorial Club Universitario, Spain, (2008).
12. R. Navarro Álvarez, bachelor's degree, Diseño por durabilidad de estructuras de concreto, Instituto Politécnico Nacional (2008) 77-78.

13. J.T. Pérez-Quiroz, J. Terán, M. J. Herrera, M. Martínez, J. Genescá, *J Construc Steel Research*, 64, 11 (2008) 1-2.
14. Knudsen, F. M. Jensen, O. Klinghoffer, T. Skovsgaard, P*roceedings of the International Conference on Corrosion and Rehabilitation of Reinforced Concrete Structures, Orlando, Florida, USA*, (1999) *15*.
15. G. Istrati, Manual de Aceros Inoxidables, Editorial Alsina (1961) 230.
16. Y. Meas, E.J. Rodríguez, J. Genescá, J. Mendoza, R. Durán, Uruchurtu, J. M. Malo, E. A. Martínez, C. Arganis, T. Pérez, A. Martínez, J. G. Chacón, C. Gaona, F. M. Almeraya, J.G. González, Técnicas electroquímicas para el control y estudio de la corrosión, UNAM, Facultad de Química, (2002).
17. F. J. Molina, G. M. Duran, bachelor's degree, Evaluación del daño por corrosión en el refuerzo del concreto en ambiente de cloruros, por las técnicas de ruido electroquímico y RPL, Universidad Industrial de Santander (2009) 19-20.
18. H. Sarmiento, J. Goellner, A. Heyn, *Ingeniería y Desarrollo*, 21 (2007) 56-72.
19. D. Cabrera, Master's degree, *Efecto del flujo turbulento en la corrosión de soldaduras de aceros de alta resistencia*, Universidad Veracruzana, (2013).
20. ASTM A615/A615M-12 Standard Specification for Deformed and Plain Carbon-Steel Bars for Concrete Reinforcement.
21. NMX-H-121-1988 Procedimiento de soldadura estructural acero de refuerzo.
22. ANSI/AWS D1.4-M 2005 Structural Welding Code — Reinforcing Steel.
23. ASTM G199-2009 Standard Guide for Electrochemical Noise Measurement.
24. ASTM E3-2011 Standard Guide for Preparation of Metallographic Specimens.
25. Metals Handbook, Metallography and microstructures, Editor G. F. Vander Voort, ASM International, 9, (2004), 1184.
26. ASTM G3-2010 Standard Practice for Conventions Applicable to Electrochemical Measurements in Corrosion Testing.
27. ASTM G5-2013 Standard Reference Test Method for Making Potentiodynamic Anodic Polarization Measurements.
28. ASTM C876-2009 Standard Test Method for Corrosion Potentials of Uncoated Reinforcing Steel in Concrete.
29. J. C. Lippold, D.J. Kotecki, Welding Metallurgy and Weldability of Stainless Steels, Wiley-VCH, (2005).
30. A.E. Ares , R. Caram, M.A. Jaime, P. Ferrandini, A.T. Dutra, S.F. Gueijman, C.E. Schvezov, *Anales AFA*, 17 (1) (2005) 240.
31. ASTM G82-2014, Standard Guide for Development and Use of a Galvanic Series for Predicting Galvanic Corrosion Performance.
32. E. Sistonen, P. Tukiainen, S. Peltola, S. kriko, M. Lastala, S. Huovinen. *Restricting Corrosion Risk in Reinforced Concrete Structures under Outdoor Conditions*,1 (2000) 47.
33. ASTM G59-2009 Standard Test Method for Conducting Potentiodynamic Polarization Resistance Measurements.
34. M. Moreno, W. Morris, M.G. Álvarez, G.S. Duffo, Proceeedings SAM 2000, IV Coloquio Latinoamericano de Fractura y Fatiga, (2000) 751-758.
35. O. TROCONIS, L. Uller, I. Alanís, P. Helene, R. Mejias, V. O´Reilly, C. Andrade, J. Carpio, I. Díaz, M. Salta, G. Rodríguez, A. Romero, A. Sagues, Manual de inspección, evaluación y diagnóstico de corrosión en estructuras de hormigón armado, *Durar, Red temática del CYTED* (1997).
36. R. G. Kelly, M. E. Inman, J. L. Hudson, Analysis of Electrochemical Noise for Type 410 Stainless Steel in Chloride Solutions, Electrochemical noise measurements for corrosion applications Jeffery R. Kearns, John R. Scully, Pierre R. Roberge, David L. Reichert, and John L. Dawson, Eds., ASTM STP 1277, (1996)101-113.

37. D. A. Eden, D. G. John, J. L. Dawson, International patent WO 87/07022. *World Intellectual Property Organization*, 19 (1987).